

VACANCY MOBILITY IN NICKEL ALUMINIDE VERSUS COMPOSITION

BIN BAI, JIAWEN FAN and GARY S. COLLINS*

Department of Physics, Washington State University, Pullman, WA 99164, *collins@wsu.edu

ABSTRACT

The fractional concentration of Ni-vacancies in NiAl at high temperature has been determined for compositions between 50 and 53 at.% Ni from measurements using perturbed angular correlation of gamma rays (PAC). The vacancies were detected by quadrupole interactions induced at nearby $^{111}\text{In}/\text{Cd}$ impurity probes present on the Al sublattice in high dilution. One set of measurements was made at high temperature. A second set made after rapid quenching exhibited an enhancement of Ni-vacancy site fractions that is attributed to diffusion and trapping of vacancies during quenching. The composition dependence of the enhancement was analyzed assuming that the enhancement is proportional to the root-mean-square diffusion length during quenching. The experimental dependence on composition is found to be consistent with bulk diffusion data. The methodology developed clarifies how local environments of impurity probes are modified during rapid quenching. In addition, it is shown that there is an enormous increase in the mobility of vacancies with increasing deviation of the composition from stoichiometry. Diffusion mechanisms that can explain the data trends are discussed.

INTRODUCTION

A number of different microscopic diffusion mechanisms have been proposed to explain diffusion data for B2 intermetallic compounds, but the situation is unclear and more than one mechanism may be important. The composition-dependence of the diffusivity in single-phase compounds such as NiAl may help identify the mechanisms, and is the subject of this paper. Below, we will consider NiAl with slightly Ni-rich compositions. Kao, Kim and Chang considered the composition dependence of two mechanisms [1]: (1) The Huntington-McCombie-Elcock (HME) 6-jump cycle, by which vacancy jump cycles lead to diffusion of atoms on both sublattices without increase in disorder. (2) The antistructure-bridge (ASB) mechanism [1], by which Ni-vacancies jump “through” Ni-antisite atoms whose concentration increases in more Ni-rich alloys. To those can be added (3) triple-defect mechanisms (TD) which are 3-jump cycles that can occur when there is a juxtaposition of Ni-antisite defects and Ni-vacancies. [2]. Finally, in addition to the foregoing near-neighbor jump mechanisms, there is (4) the next-near neighbor (NNN) mechanism in which Ni-vacancies jump on their own simple-cubic sublattice, for which support comes from recent calculations by Mishin and Farkas using the embedded atom method. [3] We will use square brackets to define the fractional concentration of a defect, for example $[V_{\text{Ni}}]$, with respect to the number of sites on one sublattice. For composition $\text{Ni}_{1+2x}\text{Al}_{1-2x}$, the deviation from stoichiometry, x , is accommodated at low temperature by placement of excess Ni atoms on the Al-sublattice (Ni_{Al}), with $[\text{Ni}_{\text{Al}}]=2x$. It has been shown by macroscopic measurements [4] and in PAC experiments [5] that the dominant equilibrium defect in NiAl at high temperature is the triple-defect. The triple-defect is the combination of two vacancies on the Ni-sublattice (V_{Ni}) and one antisite Ni_{Al} atom, all three presumably located at random.[4] It is one combination of elementary defects that preserves the local chemical composition of the alloy. If the triple-defect is the dominant thermal defect, then it can be shown [5] using the law of mass action and an equation of constraint linking the

deviation from stoichiometry, x , and defect concentrations, $[V_{Ni}] + 4x = 2[Ni_{Al}]$, that in equilibrium,

$$\frac{[V_{Ni}]^3}{2} + 2x[V_{Ni}]^2 = K_T = [V_{Ni}]^2[Ni_{Al}] = \exp(S_F / k_B) \exp(-E_F / k_B T). \quad (1)$$

Here, K_T is the equilibrium constant for formation of the triple-defect combination, with formation entropy S_F and enthalpy E_F . In stoichiometric NiAl (that is, $x=0$) at 1150C, $[V_{Ni}]$ is roughly 0.005. For compositions not too close to stoichiometry, so that $[V_{Ni}] \ll x$, the composition dependences for the different diffusion mechanisms are as given in Table I. [6]

Table I. Composition dependence of diffusion mechanisms in B2 intermetallics

Mechanism	Composition dependence
HME Huntington 6-jump cycle	$D \sim [V_{Al}] \sim x^{+1/2}$ (ref. 1)
ASB Antistructure bridge	$D \sim [V_{Al}]^3 \sim x^{+3/2}$ (ref. 1)
TD Triple-defect 3-jump cycles	$D \sim [V_{Al}][Ni_{Al}] \sim x^{+3/2}$
NNN Next-nearest neighbor	$D \sim [V_{Ni}] \sim x^{-1/2}$

The measurements reported here were made using a nuclear probe method, perturbed angular correlations of gamma rays (PAC). Point defects localized next to radioactive ^{111}In probe atoms were detected by nuclear quadrupole interactions they induce.[7,8] In early measurements on annealed samples, signals were identified with probe atoms on Al-sites having one or two Ni-vacancies in the first neighbor shell.[9] Signal amplitudes are proportional--using known conversion factors--to the fractions of the probe atoms in the different lattice sites. An attractive interaction exists between the In-probe and Ni-vacancies that enhances the presence of vacancies in the first shell. The binding enthalpy has been measured to be $E_B = 0.18(1)$ eV,[10,11,12] leading to an enhancement of the concentration c_I of vacancies in the first shells of probes by the factor $\exp(E_B / k_B T)$. Thus $c_1 = [V_{Ni}] \exp(E_B / k_B T)$ and site-fractions of In probes having zero or one Ni-vacancy in the first shell are then given in good approximation by the binomial probabilities $f_0 = (1 - c_1)^8$ and $f_1 = 8c_1(1 - c_1)^7$, in which 8 is the number of near-neighbor sites on the Ni-sublattice. Normalized by the vacancy-free site-fraction, the monovacancy site-fraction in good approximation then has the following simple form:

$$\frac{f_1}{f_0} = 8[V_{Ni}] \exp(E_B / k_B T). \quad (2)$$

PAC measurements were made in equilibrium at high temperature [5] and on rapidly quenched [10] samples having compositions in the range 50 to 53.5 at.% Ni ($x=0$ to 0.035). For the high-temperature measurements, experimental values of f_1/f_0 and the known value of E_B were inserted in eq. 2 to determine the vacancy concentration $[V_{Ni}]$. The vacancy concentration and composition parameter x were then inserted in eq. 1 to determine the equilibrium constant K_T for the known experimental values of T and x . From 12 measurements over the range $T=1070$ to 1490 K on three samples having $x=0.0003$, 0.0014 and 0.0091, a good Arrhenius behavior for K_T was obtained, with fitted values $E_F = 1.65(4)$ eV and $S_F = -3.3(4) k_B$. [5] The corresponding magnitude of the equilibrium constant K_T is in good agreement with thermodynamic activity measurements.[4] Samples were quenched by dropping them out of a vertical furnace and had a quenching rate estimated to be about 10^4 K/s.[10] For compounds like NiAl that have a low

vacancy mobility, such a rate is rapid enough to avoid annealing out of vacancies during quenching. However, local motion of vacancies near the probes during quenching is unavoidable and leads in the present situation to trapping. To analyze the site fractions, we assumed that vacancies in the probes' first shells remain in local equilibrium with a constant lattice concentration $[V_{Ni}]$ during cooling until some "freeze-in" temperature T^* is reached below which all vacancy motion is frozen out. Simple numerical estimates showed that, for an equilibration temperature of 1000 C, the freeze-in temperature would be hundreds of degrees lower. This leads to a further enhancement beyond the equilibrium enhancement factor for quenched samples, so that the normalized site fraction is $(f_1 / f_0)_Q = 8[V_{Ni}] \exp(E_B / k_B T^*)$, in which $[V_{Ni}]$ is the concentration at the equilibration temperature T prior to quenching.

EXPERIMENT

We compare site fractions from measurements at high temperature and on quenched samples as a function of x, for x in the range 0 to 0.035. Spectra of five samples measured at 1460 K are shown in Fig. 1.[4] The signal having a period of about 53 ns in the figure is the monovacancy signal.[9] As can be seen, the signal amplitude (site fraction) falls off as x increases, in accord with eq. 1. Normalized site fractions obtained from the fitted amplitudes of the spectra are shown in Fig. 2. Excluding the data point at x=0.0003, a power-law fit of the concentration dependence of the site fraction yielded $f_1/f_0 \sim x^{-0.4(1)}$, in agreement with $x^{-1/2}$ expected according to the triple-defect model (cf. eq. 1 and 2 for $x \gg [V_{Ni}]$). Site fractions for 7 samples quenched all in the same way from 1320 K are shown in Fig. 3.

RESULTS

Comparison of Fig. 2 and 3 shows two major differences: (1) The site-fractions for quenched samples are enhanced by a factor of about ten, which we attribute to diffusion and trapping during quenching as described above. (2) The enhancement increases with x, indicating that the mobility of the vacancies increases with x. For a detailed comparison of the two data sets, an adjustment needs to be made to take into account the somewhat different equilibration temperatures for the data in Figs. 2 and 3. This was done by dividing values of $(f_1/f_0)_Q$ by the equilibrium site fraction (f_1/f_0) at 1320 K calculated under the triple-defect model using eq. 1 and 2 and the experimental values given above for E_F , S_F and E_B .

In Fig. 4 is shown the ratio $(f_1/f_0)_Q/(f_1/f_0)$ as a function of x. As can be seen, the enhancement due to quenching varies from 5 near stoichiometry to 12 at x= 0.035. The curve in Fig. 4 is the result of a fit of the composition dependence of the data to an exponential function $a \exp(bx)$, from which the enhancement at stoichiometry, $a= 4.8(2)$, and coefficient $b= 26(6)$ were obtained. From the enhancement at stoichiometry, the freeze-in temperature $T^* = T / (1 + \ln(a) \cdot k_B T / E_B)$, or $T^*= 660$ K for $T= 1320$ K, a very low value. Assuming Newton's law of cooling with a fixed relaxation time, T^* is independent of composition.

To interpret the composition dependence, we suppose that the probability for trapping vacancies is proportional to the rms diffusion distance during quenching. This means that $(f_1/f_0)_Q/(f_1/f_0)$ should be proportional to the square root of the diffusivity, and that the diffusivity should vary as $\exp(2bx) = \exp(52(12) x)$. To test the supposition, we determined the corresponding composition dependence of the diffusivity D of Ni from the literature. From Fig.

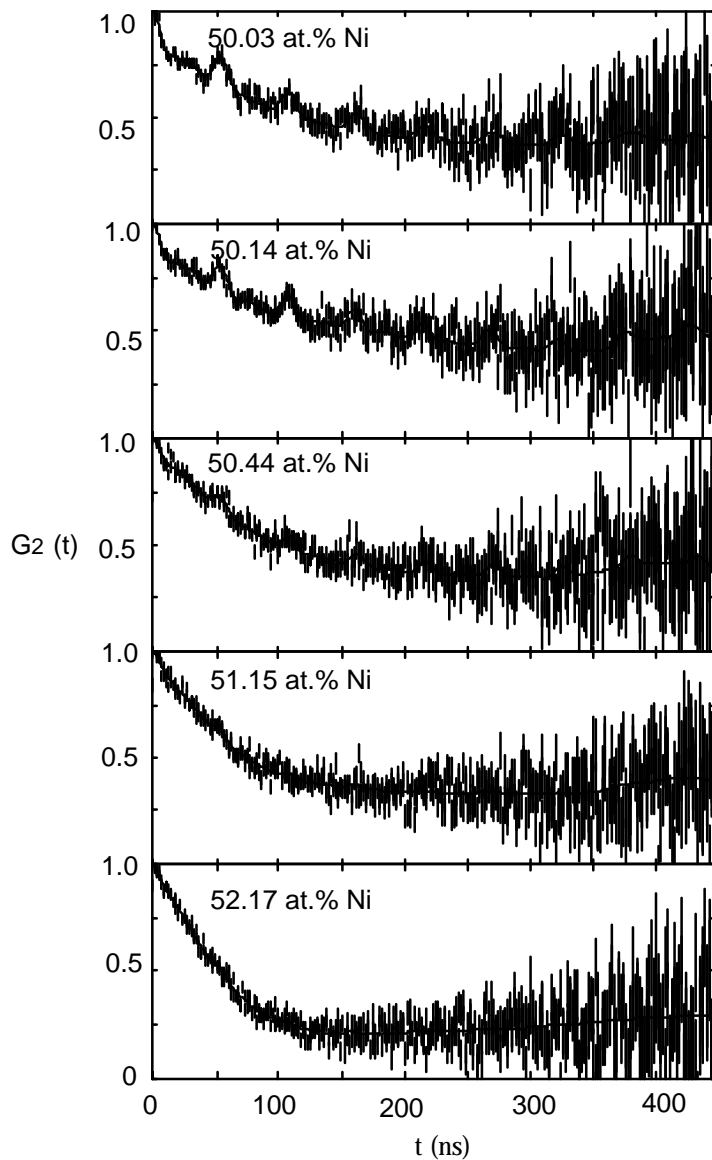


Fig. 1. PAC spectra of NiAl of different compositions, all measured at 1460 K. The signal with period 53 ns is due to a single Ni-vacancy in the near-neighbor shell of PAC probe atoms.

predicted diffusivities whose curvatures with respect to x are positive, as observed experimentally. Indeed, the enhancement factors shown in Fig 4 yield a linear trend when plotted versus $x^{+3/2}$, just like the dependences listed in Table I. Thus, the ASB and/or TD mechanisms appear to dominate the diffusivity, but close to stoichiometry, where the ASB and TD mechanisms are ineffective, the NNN and HME mechanisms may contribute appreciably.

Most remarkable, however, is the rapid increase in the vacancy mobility with x . Over the range $x=0$ to 0.035, the diffusivity increases by a factor of 6 while, from eq. 1, the vacancy concentration $[V_{Ni}]$ decreases by a factor of 5. This implies an increase in the mobility of vacancies by a factor of $D/[V_{Ni}] \sim 30$.

15 of Shankar and Seigle,[13] diffusion data at 1370 K over the range 50-56 at.% Ni yielded $D_{Ni} \sim \exp(50x)$ whereas data by Hancock and McDonnell shown in the same figure yielded $D_{Ni}^* \sim \exp(40x)$. The good agreement between our measured dependence, $\exp(52x)$, and diffusion data supports our method of analysis of vacancy site fractions in quenched samples using impurity hyperfine probes. The same approach should be useful for other microscopic methods such as Mössbauer effect.

What diffusion mechanism(s) can lead to the increase in diffusivity with x observed both in diffusion data and our microscopic measurements? Since the equilibrium site fraction is proportional to the vacancy concentration $[V_{Ni}]$, the decrease with x shown in Fig. 2 demonstrates unambiguously that the Ni-vacancy concentration decreases rapidly with x . This is in accord with the triple-defect model for the equilibrium defect (eq. 1), but the rapid decrease makes the increase in the diffusivity with x all the more surprising. Of the four diffusion mechanisms listed on Table I, the NNN diffusion mechanism can be ruled out as the dominant mechanism over the range 50 to 54 at.% Ni because it has the wrong dependence on x . Of the others, the ASB and TD mechanisms have

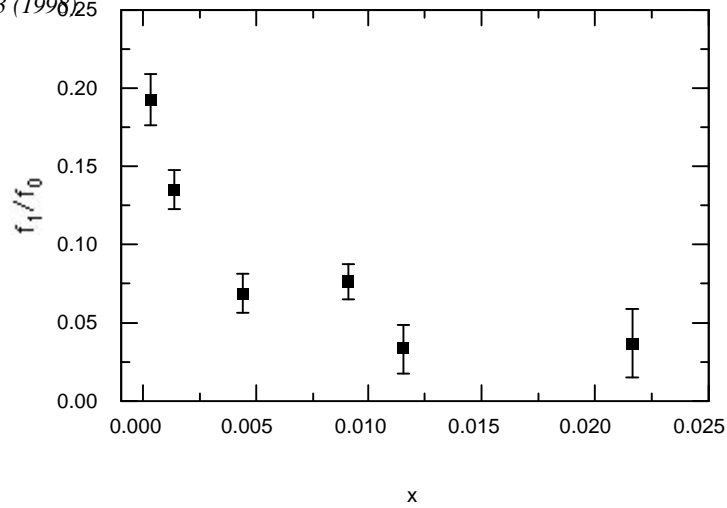


Fig. 2. Monovacancy site fractions in NiAl measured at 1460 K versus the deviation from stoichiometry.

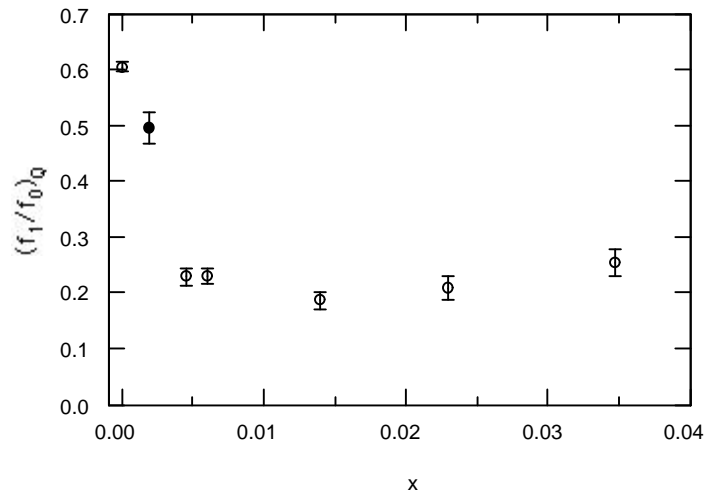


Fig. 3. Monovacancy site fractions in NiAl measured after quenching from 1320 K.

CONCLUSIONS

By directly observing a microscopic signal whose amplitude is proportional to the fractional concentration of Ni-vacancies, PAC measurements support the conclusion from thermodynamic activity measurements that the equilibrium high-temperature defect in NiAl is the triple defect ($2V_{\text{Ni}} + \text{Ni}_{\text{Al}}$). A methodology was developed to explain a large enhancement of vacancy site fractions observed after quenching. The methodology involves the concept of a freeze-in temperature during quenching below which all vacancy motion is frozen out. The composition dependence of the enhancement correlates well with diffusion data. An enormous increase in the mobility of vacancies is correlated with increasing Ni content.

ACKNOWLEDGMENT

This work was supported in part by the National Science Foundation under grant DMR 96-12306 (Metals Program) and predecessor grants.

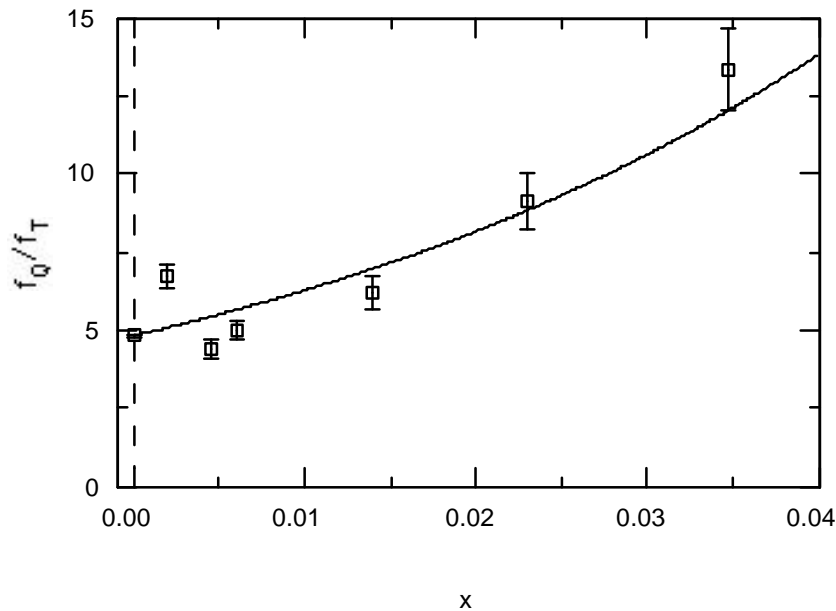


Fig. 4. Enhancement of normalized monovacancy site-fraction in NiAl at 1320 K as a function of composition.

REFERENCES

1. C.R. Kao, Sungtae Lee and Y.A. Chang, *Mat. Sci. & Engin.* A192/193, 965 (1995).
2. Jean Philibert, *Atom movements: diffusion and mass transport in solids*, translated by Steven J. Rothman (Les Editions de Physique, 1991), pp. 187-191.
3. Yuri Mishin and Diana Farkas, *Phil. Mag.* A75, 169 and 187 (1997).
4. Y. Austin Chang and Joachim P. Neumann, *Prog. Solid State Chem.* 14, 221 (1982) and references therein.
5. Bin Bai, Ph.D. dissertation, Washington State University 1997 (unpublished).
6. The first three mechanisms all involve very low equilibrium concentrations of Al-vacancies present, for example, due to thermal formation of Schottky vacancy pairs.
7. E. Recknagel, G. Schatz and Th. Wichert, in *Hyperfine Interactions of Radioactive Nuclei*, ed. J. Christiansen, p. 133 (Springer, 1983).
8. G.S. Collins, S.L. Shropshire and J. Fan, *Hyperfine Interactions* 62, 1 (1990).
9. J. Fan and G.S. Collins, *Hyperfine Interactions* 60, 655 (1990).
10. J. Fan, Ph.D. dissertation, Washington State University, 1992 (unpublished), and ref. [8*].
11. G.S. Collins, J. Fan and B. Bai, in *Structural Intermetallics 1997*, ed. M.V. Nathal et al., (The Minerals, Metals and Materials Society, 1997), p. 43.
12. The measurement of the binding enthalpy was made in an unusual low-temperature regime in NiAl extending between about 350 and 650 C in which quenched-in excess Ni-vacancies are able to diffuse without annealing out (cf. ref. 10 and 11).
13. S. Shankar and L.L. Seigle, *Metallurgical Transactions* 9A, 1467 (1978).